Science Academique
https://scienceacademique.com/

Science Academique
ISSN 2583-6889
Benny D and Prasana JC.
Pages: 47-68

Research Article

Density functional theory studies, experimental investigations (FT IR, FT Raman), *in vitro* assay studies and molecular docking studies on 3-acetamidotetrahydro-2-thiophenone

Dona Benny, Johanan Christian Prasana*

Department of Physics, Madras Christian College, East Tambaram, Chennai, 600059, Tamilnadu, India

***Correspondence to:** Johanan Christian Prasana; reachjcp@gmail.com

Citation: Benny D, Prasana JC (2025) Density functional theory studies, experimental investigations (FT IR, FT Raman), in vitro assay studies and molecular docking studies on 3-acetamidotetrahydro-2-thiophenone. *Sci Academique* 6(1): 47-68

Received: 10 March, 2025; **Accepted:** 7 April, 2025; **Published:** 16 April, 2025

Abstract

This work investigates the compound, 3-Acetamidotetrahydro-2-thiophenone computationally, and obtained results are compared experimentally. Given its efficiency and cost-effectiveness, DFT calculations (B3LYP functional) with a suitable basis set were utilized to determine stable, minimum-energy structure of the compound. Experimental and theoretical FT-IR and FT-Raman spectra were compared. To elucidate electronic properties, various theoretical studies were conducted. Additionally, topological analysis was performed to assess molecular structure. To evaluate potential biological activity, drug-likeness, and molecular docking studies were carried out. *In vitro* cytotoxicity assays were conducted. Results suggest that 3-acetamidotetrahydro-2-thiophenone exhibits anti-emphysema and holds promise as a potential therapeutic agent for emphysema.

Keywords: Dft; Thiophenone moiety; Vibrational assignments; Molecular docking; *In vitro* assay studies

Introduction

Thiophene has emerged as a prospective entity in the rapidly expanding field of heterocyclic compounds with its intriguing pharmacological properties [1]. Thiophene is a heteroaromatic molecule with five members and one sulphur atom. Thiophene derivatives are significant heterocycles in medicinal chemistry that have remarkable applications [2]. Thiophene

Science Academique
ISSN 2583-6889
Benny D and Prasana JC.
Pages: 47-68

derivatives exhibit anticancer action [3], antihypertensive [4], analgesic and anti-inflammatory [5], and antibacterial [6] activities. Tetrahydrothiophene is also termed as Thiophane which is a saturated thiophene [7]. Since nitrogen heterocycles have been thoroughly studied in medicinal chemistry, researchers' focus has switched to other heterocycles, particularly S-heterocycles. Compounds containing S-heterocycles have been widely documented to have anti-inflammatory, anti-cancer, anti-diabetic, antibacterial, antihypertensive, and antiviral properties up to this point. Raloxifene, is a heterocyclic compound with sulphur that has FDA approval and is used as a popular medication for breast cancer. Thiabendazole is an antifungal medication. Rosiglitazone is clinically used to treat diabetes, clopidogrel is used to treat peripheral artery diseases and ritonavir is a strong antiviral agent [8].

Thiophene moiety has acquired attention for its diverse applications. This study focuses on 3-acetamidotetrahydro-2-thiophenone ($C_6H_9NO_2S$) of Molecular weight 159.20 g/mol. The title compound has not been previously investigated using DFT or molecular docking. To analyze potential applications of this compound, conducted a comprehensive analysis involving structural characterization, spectroscopic analysis, and biological evaluation. DFT studies were done to elucidate the molecular structure of 3-acetamidotetrahydro-2-thiophenone. Additionally, theoretical and experimental spectroscopic analyses were performed to validate structural, electronic information. To assess the compound's biological potential and pharmaceutical relevance, biological assays were conducted.

Experimental Details

3-acetamidotetrahydro-2-thiophenone compound was obtained from Tokyo Chemical Industry Co., Ltd., with a purity exceeding 98%. Experimental analyses, including FT-IR, FT-Raman, were conducted at the SAIF, IIT Madras. FT-IR spectrum (4000-400 cm^{-1}) was recorded using KBr pellet preparation. FT-Raman spectrum (4000-100 cm^{-1}) was obtained. *In vitro* cytotoxicity and biological activity of 3-acetamidotetrahydro-2-thiophenone were evaluated against the human lung carcinoma (A549) cell line at Radiant Research Services Pvt. Ltd., Bangaluru, India.

Computational Details

DFT calculations using Gaussian 16W [9] and GaussView 05 [10] software packages were performed [9, 10]. 6-311G++(d,p) is the basis set employed. Vibrational frequency analysis was conducted using VEDA software [11]. Wavefunction analysis was performed using Multiwfn 3.8 software [12]. Drug-likeness properties were evaluated using the online SwissADME program. To assess the bioactivity of 3-acetamidotetrahydro-2-thiophenone, the PASS online tool was utilized [13]. Molecular docking using Autodock Tools 1.5.6, and visualization using Discovery Studio was carried out [14, 15].

Results and Discussion

Molecular Geometry

Science Academique
ISSN 2583-6889
Benny D and Prasana JC.
Pages: 47-68

Optimized structure of 3-acetamidotetrahydro-2-thiophenone, corresponding to a highly stable, minimum-energy conformation, was determined using DFT. Bond lengths, bond angles of headline compound were calculated, and optimized geometry is presented in figure. 1 and Table 1 [16]. Maximum bond length was observed between sulphur and carbon atoms might be due to the larger size of sulphur than the carbon atoms surrounded. S1–C7 bond exhibited the maximum bond length of 1.815 Å and S1-C8 is 1.765 Å. Carbon-carbon bonds in the ring structure are found to be 1.5 Å. There are two carbon-oxygen bonds, O2-C8, and O3-C9, which exhibit bond lengths of 1.221 and 1.227 Å respectively. N4-H16 bond was the shortest, measuring 1.017 Å. Largest bond angle identified was 126.3° between O2-C8-C5. Smallest bond angle, 93.8°, was observed between C7-S1-C8 atoms [17].

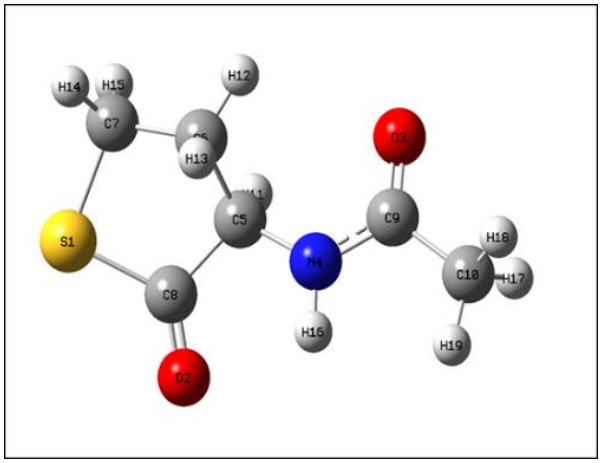

Figure 1: Optimized structure of 3-Acetamidotetrahydro-2-thiophenone.

PARAMETER	Values
BOND LENGTH(Å)	
S1-C7	1.815
S1-C8	1.765
O2-C8	1.221
O3-C9	1.228
N4-C5	1.434
N4-C9	1.391
N4-H16	1.017
C5-C6	1.525
C5-C8	1.51
C5-H11	1.096
C6-C7	1.518
C6-H12	1.096
C6-H13	1.099
C7-H14	1.093
C7-H15	1.094
C9-C10	1.505

Science Academique
ISSN 2583-6889
Benny D and Prasana JC.
Pages: 47-68

C10-H17	1.094
C10-H18	1.093
C10-H19	1.094
Bond angle (◦)	
C7-S1-C8	93.8
S1-C7-C6	103.7
S1-C7-H14	111.2
S1-C7-H15	109.3
S1-C8-O2	123
S1-C8-C5	110.6
O2-C8-C5	126.3
O3-C9-N4	125.5
O3-C9-C10	121.8
C5-N4-C9	123.6
C5-N4-H16	118
N4-C5-C6	112.3
N4-C5-C8	109.2
N4-C5-H11	110.1
C9-N4-H16	118.4
N4-C9-C10	112.6
C6-C5-C8	106
C6-C5-H11	110.7
C5-C6-C7	107.3
C5-C6-H12	111.2
C5-C6-H13	110.8
C8-C5-H11	108.5
C7-C6-H12	111.1
C7-C6-H13	110
C6-C7-H14	112.1
C6-C7-H15	111.2
H12-C6-H13	106.5
H14-C7-H15	109.2
C9-C10-H17	109.7
C9-C10-H18	109.4
C9-C10-H19	110.4
H17-C10-H18	109.3
H17-C10-H19	108.6
H18-C10-H19	109.5

Table 1: Optimized molecular geometry of 3-Acetamidotetrahydro-2-thiophenone.

Vibrational Analysis

Vibrational spectroscopy is a valuable tool for identifying functional groups within molecules.

Science Academique
ISSN 2583-6889
Benny D and Prasana JC.
Pages: 47-68

3-acetamidotetrahydro-2-thiophenone has 51 vibrational modes (3n-6). This study compares experimental (FT-IR, FT-Raman) with theoretical spectra. Calculated frequencies were scaled (0.961) to improve agreement with experimental data. Theoretical and experimental spectra exhibit excellent correlation, as shown in Figures 2, 3. Vibrational assignments are listed in Table 2 [18]. N-H stretching vibration creates a band between 3500 and 3300 cm^{-1} [19]. A peak at 3447 cm^{-1} was obtained theoretically. C-H stretching vibrations are present in the 3000–3100 cm^{-1} range [20]. At 3016 cm^{-1}, FT IR experimental peak was seen and at 3015 cm^{-1}, FT Raman peak was seen. Theoretical peak was also within the range. Desired region of C-O stretching is between 1740 to 1660 cm^{-1} [21]. Experimental FTIR peaks are at 1761 and 1692 cm^{-1}. FT Raman (exp) peaks were seen at 1693, 1652 cm^{-1}. Theoretically obtained peaks (1705, 1670 cm^{-1}) are also within the range [22].

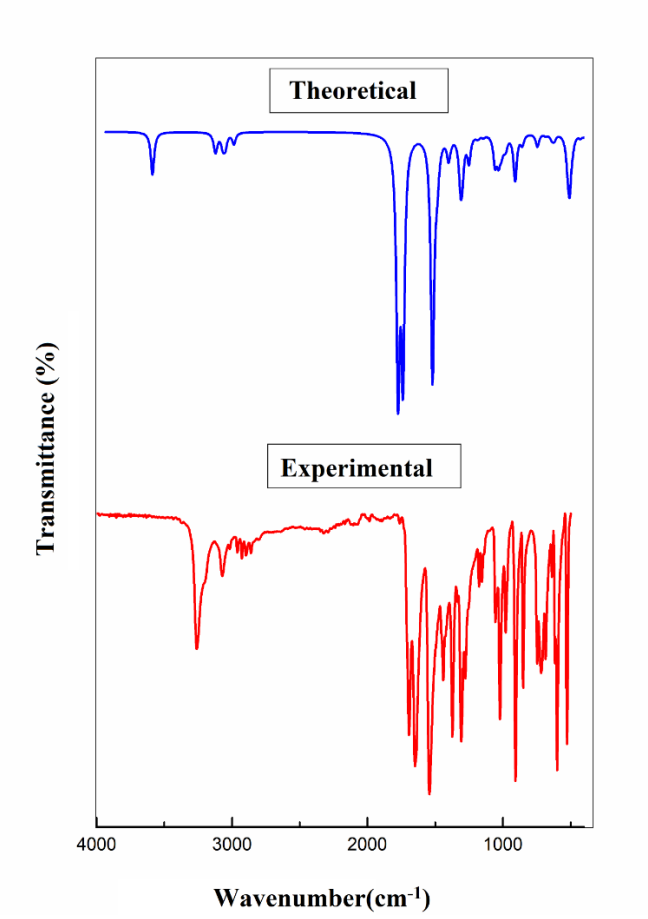

Figure 2: FT-IR spectra of 3-Acetamidotetrahydro-2-thiophenone.

Science Academique
ISSN 2583-6889
Benny D and Prasana JC.
Pages: 47-68

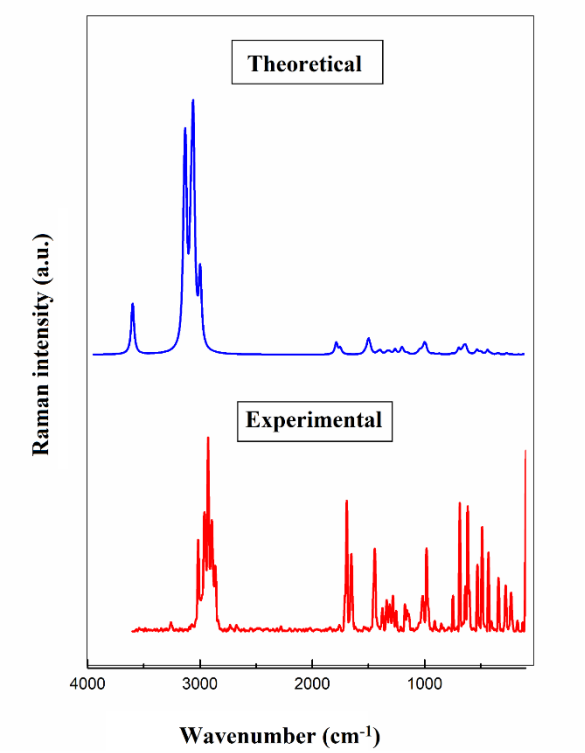

Figure 3: FT-Raman spectra of 3-Acetamidotetrahydro-2-thiophenone.

Modes	Exp FTIR	Exp FTR	unscaled	scaled	abs	rel	abs	rel	Vibrational assignents
51			3587	3447	17	57	36	64	ϒ NH (100)
50	3016	3015	3129	3007	2	6	45	81	ϒ CH (90)
49			3122	3000	4	14	33	58	ϒ CH (90)
48			3117	2995	1	5	41	73	ϒ CH (97)
47			3115	2993	1	4	48	85	ϒ CH (100)
46	2959	2959	3068	2948	5	17	59	105	ϒ CH (96)
45			3052	2933	4	12	53	94	ϒ CH (97)
44		2927	3045	2927	2	6	100	178	ϒ CH (99)
43		2825	2985	2869	5	15	51	91	ϒ CH (98)
42	1761	1693	1774	1705	100	329	8	15	ϒ CO (92)
41	1692	1652	1738	1670	93	306	4	8	ϒ CO(82)
40	1542		1520	1461	98	324	1	2	ϒ NC (22)+β HNC(50)
39	1440	1445	1501	1442	1	2	2	3	β HCH(92)
38			1490	1431	2	7	6	11	β HCH(85)
37			1486	1428	11	36	3	5	β HCH(68)+ τ HCCN (21)
36			1473	1416	2	8	4	6	β HCH(80)+ τ HCCN (13)
35	1372	1376	1401	1346	9	29	1	2	β HCH(87)

Science Academique
ISSN 2583-6889
Benny D and Prasana JC.
Pages: 47-68

34	1334	1338	1381	1327	1	3	2	4	β HCN(16)+τ HCCS (52)
33	1277	1282	1323	1271	1	5	1	3	β HCN(17)+τ HCCS (45)+τ HCSC (11)
32			1311	1260	18	60	1	1	β HCC(22)+τ HCCS (24)
31			1299	1248	11	35	1	3	τ HCSC (42)
30			1250	1202	11	35	3	6	ϒ NC (14)+β HNC(22)+β HCN(21)
29		1174	1191	1145	1	2	4	7	β HCS(27)+β HCN(13)+β HCC(16)
28	1176		1180	1134	1	3	2	3	ϒ NC (37)+ϒ CC (14)
27			1145	1100	1	3	1	2	β HCC(14)+τ HCCS (10)+τ HCSC (12)
26		1017	1059	1018	9	30	0	0	ϒ CC (30)+β HCS(24)+β HCN(10)
25	1054		1056	1015	2	7	0	0	β HCH(24)+τ HCCN (54)+ω OCNC (16)
24	1021		1032	992	9	31	3	5	β HCS(13)
23		983	1012	972	6	19	1	3	τ HCCN (35)
22			991	952	3	8	6	10	ϒ CC (30)
21	979		977	939	4	13	4	8	ϒ CC (60)
20	906		910	874	19	62	1	1	ϒ CC (16)+β OCS(11)+τ HCCS (10)
19	850		857	823	4	13	1	1	β HCS(11)+τ HCSC (28)+τ HCCS (11)
18	746	748	745	716	5	18	1	1	ϒ CC (26)+ϒ SC (16)+ω OCSC (12)
17	684	687	684	657	1	3	4	7	β CCC(27)+β SCC(24)
16		638	653	628	0	1	1	2	τ CCCC (12)+ω OCSC (13)+ω OCNC (14)
15	637	617	637	613	2	7	4	7	ω OCNC (35)
14	614		620	596	2	8	5	8	ϒ CC (12)+β CCC(16)+ω OCSC (24)+ω OCNC (14)
13	526	539	522	501	9	28	3	6	β OCC(40)+β CCC(16)
12		488	507	488	21	69	0	0	τ HNCC (81)
11			486	467	3	8	2	3	β OCS(13)+β OCC(10)+β SCC(39)
10		432	427	410	1	5	3	6	ϒ SC (43)+β OCS(38)
9			400	384	1	4	1	1	β CCC(10)+ω OCSC (28)+ω NCCC (29)
8		342	334	321	0	1	1	2	β CCN(43)+β CCN(12)
7		279	257	247	0	1	1	2	β OCS(11)+β OCC(10)+β CNC(11)+β NCC(22)
6		231	217	208	1	2	0	0	β CCC(10)+β CNC(10)+τ HCCS (12)+τ CCCC (29)
5			150	144	2	7	0	0	β CNC(25)+τ CCNC (12)+τ SCCC (21)
4		92	106	101	3	10	0	1	β CNC(15)+β NCC(28)+τ CCNC (23)

Science Academique
ISSN 2583-6889
Benny D and Prasana JC.
Pages: 47-68

3		71	84	81	1	5	0	1	τ HCCN (10)+τ CCNC (24)+τ SCCC (32)+ωNCCC(11)
2			61	58	3	9	0	1	τ HCCN (37)+τ CNCC (28)+τ CCNC (19)+ω OCNC (10)
1			52	50	1	2	0	0	τ HCCN (20)+τ CNCC (58)
ϒ- stretching, β – In plane bending, ω – Out of plane bending, τ – Torsion. *Scaling factor 0.961 for B3LYP/6-311++G(d,p) basis set. ** Normalised to 100.									

Table 2: Experimental and calculated vibrational spectroscopic data with vibrational assignments on 3-Acetamidotetrahydro-2-thiophenone.

FMO

Molecular orbitals, particularly HOMO and LUMO, provide valuable insights into bioactivity of a molecule. The HOMO-LUMO energy gap is a key indicator of a molecule's stability and reactivity. A smaller HOMO-LUMO gap generally correlates with higher reactivity, while a larger gap suggests greater stability [23-26]. Table 3 presents global chemical parameters of 3-acetamidotetrahydro-2-thiophenone, and Figure 4 illustrates HOMO-LUMO transitions. Gas-phase HOMO-LUMO energy gap is 6.088 eV. Furthermore, chemical softness and hardness values were calculated using global chemical parameters. Title compound exhibits increased stability due to its higher chemical hardness(3.044) and lower chemical softness (0.164) values. These results indicate that 3-acetamidotetrahydro-2-thiophenone is stable.

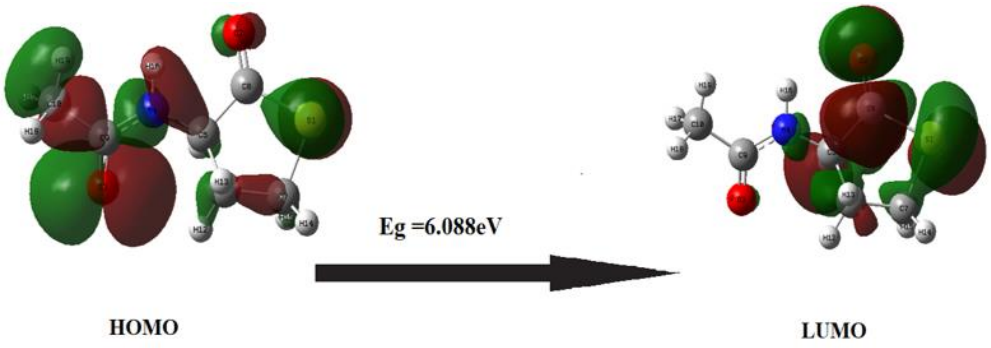

Figure 4: Frontier molecular orbital of 3-Acetamidotetrahydro-2-thiophenone.

Parameter	Values
HOMO (eV)	-7.365
LUMO (eV)	-1.278
Ionization potential	7.365
Electron affinity	1.278
Energy gap(eV)	6.088
Electronegativity	4.321
Chemical potential	-4.321

Science Academique
ISSN 2583-6889
Benny D and Prasana JC.
Pages: 47-68

Chemical hardness	3.044
Chemical softness	0.164
Electrophilicity index	3.068

Table 3: Calculated energy values 3-Acetamidotetrahydro-2-thiophenone.

Molecular Electrostatic Potential

MEP map provides a three-dimensional, color-coded representation of electron density distribution and is applied to understanding electronic structure and reactivity of a molecule [27]. MEP highlights regions of high and low electron density, identifying potential electron-donor and acceptor sites. Regions in red on the MEP map indicate areas of electrophiles, while blue regions represent areas of nucleophiles. Green regions represent neutral areas. Figure 5 presents the MEP map for 3-acetamidotetrahydro-2-thiophenone. MEP scale ranges from -5.303e-2 to 5.303e-2. [28] Oxygen atoms (O2, 03) are seen in red color which is on the negative side of the scale showing its affinity for electrons. Other atoms are seen in neutral (green) and almost neutral regions in the MEP scale indicating the zero potential.

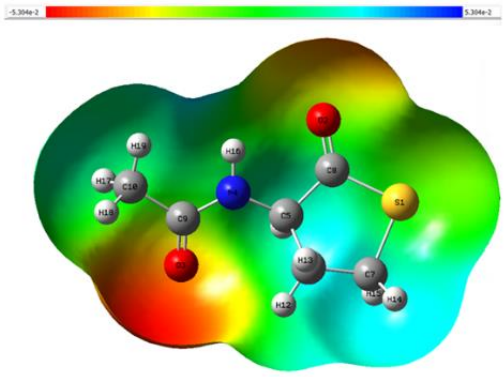

Figure 5: Molecular electrostatic potential of 3-Acetamidotetrahydro-2-thiophenone.

Non-Linear Optical Activity

Nonlinear optical (NLO) materials have significant potential applications in various fields, including medicine. NLO activity arises from interaction between electromagnetic fields and molecules. This study investigated NLO properties of 3-acetamidotetrahydro-2-thiophenone given in Table 4. Hyperpolarizability component is a key indicator of NLO activity in organic molecules. Compounds with higher hyperpolarizabilities are more likely to be effective NLO materials. Calculations were performed for x, y, and z components of Dipole moment, Polarizability, and First-order hyperpolarizability.

Science Academique
ISSN 2583-6889
Benny D and Prasana JC.
Pages: 47-68

parameters	Values
βxxx	46.72
βxxy	26.32
βxyy	-9.59
βyyy	10.70
βzxx	-21.43
βxyz	2.486
βzyy	19.83
βxzz	41.36
βyzz	3.601
βzzz	32.167
βtot (a.u)	**93.513**
βtot (e.s.u)	**8.07 E-31**
α xx	128.90
α xy	-4.64
α yy	104.82
α xz	0.616
α yz	2.597
α zz	74.957
α (a.u)	**102.89**
α (e.s.u)	**1.52E-23**
Δ α (a.u)	**228.11**
Δ α (e.s.u)	**3.38E-23**
μx	0.07
μy	-0.35
μz	0.50
μ (D)	**0.62**

Table 4: Predicted dipole moment, polarizability, and first hyperpolarizability for 3-Acetamidotetrahydro-2-thiophenone.

Results show that 3-acetamidotetrahydro-2-thiophenone has a dipole moment of 0.62 (D), a polarizability of 102.89 atomic units (a.u), and a hyperpolarizability of 93.513 a.u. Notably, hyperpolarizability of 3-acetamidotetrahydro-2-thiophenone is significantly higher than that of urea, a commonly used reference molecule. These findings suggest that title compound exhibits promising NLO activity [29,30].

NBO Analysis

Natural bond orbital analysis was conducted to explore conjugative interactions or charge transfer in molecular systems. Using DFT, NBO analysis was carried out on title molecule to identify intramolecular rehybridization and delocalization of electron density in a molecule. Magnitude of stabilization energy reflects strength of the overall bonding structure and the molecule's ability to donate electrons to acceptors. Table 5 summarizes NBO parameters.

Science Academique
ISSN 2583-6889
Benny D and Prasana JC.
Pages: 47-68

Highest observed stabilization energy of 32.31 kcal/mol occurs between S1 lone pair (LP 2) donor and O2-C8 acceptor. Stabilization energies of 1.01 kcal/mol were found between S1 (acceptor) and C5-C8 (donor), and 1.02 kcal/mol between S1 (acceptor) and C5-C7 (donor) [31,32].

Donor	type	ED/e(q_i)	Acceptor	type	ED/e(q_i)	E(2)	E(j)-E(i)	F(i,j)
S1 - C 7	σ	1.98	O2 - C 8	π	0.013	4.64	1.19	0.067
S 1 - C 7	σ	1.98	C 6 - H 12	π	0.014	1.99	1.01	0.04
S 1 - C 8	σ	1.979	N 4 - C 5	π	0.029	1.67	1	0.036
S 1 - C 8	σ	1.979	C 7 - H 14	π	0.014	0.67	1.04	0.024
O 2 - C 8	σ	1.997	C 5 - C 8	π	0.077	0.75	1.48	0.03
O 2 - C 8	σ*	1.991	C 5 - C 6	π	0.024	0.5	0.77	0.018
O 2 - C 8	σ*	1.991	C 5 - H 11	π	0.031	1.62	0.78	0.032
O 3 - C 9	σ	1.992	N 4 - C 9	π	0.074	0.77	1.42	0.03
O 3 - C 9	σ	1.992	N 4 - H 16	π	0.021	0.99	1.36	0.033
O 3 - C 9	σ	1.992	C 9 - C 10	π	0.054	1.13	1.34	0.035
O 3 - C 9	σ*	1.99	O 3 - C 9	π*	0.238	1.31	0.56	0.026
O 3 - C 9	σ*	1.99	N 4 - H 16	π	0.021	0.85	0.86	0.024
O 3 - C 9	σ*	1.99	C 10 - H 17	π	0.0051	0.55	0.86	0.019
O 3 - C 9	σ*	1.99	C 10 - H 18	π	0.0052	0.69	0.86	0.022
N 4 - C 5	σ	1.982	S 1 - C 8	π	0.118	1.79	0.93	0.037
N 4 - C 5	σ	1.982	N 4 - C 9	π	0.074	1.09	1.23	0.033
N 4 - C 5	σ	1.982	C 5 - C 6	π	0.024	0.51	1.13	0.021
N 4 - C 5	σ	1.982	C 6 - C 7	π	0.012	0.73	1.12	0.026
N 4 - C 5	σ	1.982	C 9 - C 10	π	0.054	2.15	1.15	0.045
N 4 - C 9	σ	1.989	O 3 - C 9	π	0.053	0.65	1.35	0.027
N 4 - C 9	σ	1.989	N 4 - C 5	π	0.029	1.29	1.18	0.035
N 4 - C 9	σ	1.989	C 5 - C 8	π	0.077	0.87	1.17	0.029
N 4 - H 16	σ	1.982	O 3 - C 9	π	0.053	3.03	1.19	0.054
N 4 - H 16	σ	1.982	O 3 - C 9	π*	0.238	2.01	0.76	0.037
N 4 - H 16	σ	1.982	C 5 - C 6	π	0.024	1.18	1.02	0.031
N 4 - H 16	σ	1.982	C 5 - C 8	π	0.077	0.58	1.01	0.022
C 5 - C 6	σ	1.97	O 2 - C 8	π	0.013	2.89	1.23	0.053
C 5 - C 6	σ	1.97	O 2 - C 8	π*	0.233	1.26	0.62	0.026
C 5 - C 6	σ	1.97	N 4 - C 5	π	0.029	0.53	0.98	0.02
C 5 - C 6	σ	1.97	N 4 - H 16	π	0.021	1.41	1.03	0.034
C 5 - C 6	σ	1.97	C 5 - C 8	π	0.077	0.57	0.97	0.021
C 5 - C 6	σ	1.97	C 5 - H 11	π	0.031	0.56	1	0.021
C 5 - C 6	σ	1.97	C 6 - C 7	π	0.012	0.52	0.98	0.02
C 5 - C 6	σ	1.97	C 6 - H 12	π	0.014	0.59	1.04	0.022

Science Academique
ISSN 2583-6889
Benny D and Prasana JC.
Pages: 47-68

C 5 - C 6	σ	1.97	C 7 - H 14	π	0.014	1.47	1.02	0.035
C 5 - C 8	σ	1.975	O 2 - C 8	π	0.013	0.85	1.26	0.029
C 5 - C 8	σ	1.975	N 4 - C 9	π	0.074	2.58	1.12	0.049
C 5 - C 8	σ	1.975	C 5 - C 6	π	0.024	0.86	1.02	0.026
C 5 - C 8	σ	1.975	C 6 - H 12	π	0.014	1.56	1.08	0.037
C 5 - H 11	σ	1.952	O 2 - C 8	π	0.013	0.68	1.12	0.025
C 5 - H 11	σ	1.952	O 2 - C 8	π*	0.233	6.17	0.5	0.052
C 5 - H 11	σ	1.952	N 4 - H 16	π	0.021	1.06	0.92	0.028
C 5 - H 11	σ	1.952	C 6 - H 13	π	0.014	2.73	0.91	0.045
C 6 - C 7	σ	1.982	S 1 - C 8	π	0.118	0.63	0.8	0.021
C 6 - C 7	σ	1.982	N 4 - C 5	π	0.029	3.43	0.99	0.052
C 6 - C 7	σ	1.982	C 5 - C 6	π	0.024	0.53	1	0.021
C 6 - H 12	σ	1.973	S 1 - C 7	π	0.02	3.63	0.64	0.043
C 6 - H 12	σ	1.973	C 5 - C 8	π	0.077	2.21	0.85	0.039
C 6 - H 13	σ	1.979	N 4 - C 5	π	0.029	0.55	0.86	0.019
C 6 - H 13	σ	1.979	C 5 - H 11	π	0.031	2.59	0.88	0.043
C 6 - H 13	σ	1.979	C 7 - H 14	π	0.014	0.52	0.91	0.019
C 6 - H 13	σ	1.979	C 7 - H 15	π	0.022	2.45	0.9	0.042
C 7 - H 14	σ	1.986	C 5 - C 6	π	0.024	1.9	0.9	0.037
C 7 - H 15	σ	1.987	C 6 - H 13	π	0.014	2.39	0.93	0.042
C 9 - C 10	σ	1.983	O 3 - C 9	π	0.053	0.78	1.17	0.027
C 9 - C 10	σ	1.983	N 4 - C 5	π	0.029	4.04	0.99	0.057
C 10 - H 17	σ	1.976	O 3 - C 9	π*	0.238	3.05	0.61	0.041
C 10 - H 17	σ	1.976	N 4 - C 9	π	0.074	1.83	0.97	0.038
C 10 - H 18	σ	1.975	O 3 - C 9	π*	0.238	3.53	0.61	0.044
C 10 - H 18	σ	1.975	N 4 - C 9	π	0.074	1.68	0.97	0.037
C 10 - H 19	σ	1.988	O 3 - C 9	π	0.053	4.34	1.05	0.061
C 10 - H 19	σ	1.988	O 3 - C 9	π*	0.238	1.15	0.62	0.025
C 10 - H 19	σ	1.988	N 4 - C 9	π	0.074	0.52	0.98	0.021
S 1	LP (1)	1.985	C 5 - C 8	π	0.077	1.86	1.01	0.039
S 1	LP (1)	1.985	C 6 - C 7	π	0.012	0.65	1.02	0.023
S 1	LP (2)	1.766	O 2 - C 8	π*	0.233	32.31	0.24	0.079

Table 5: Second order perturbation theory analysis of Fock matrix in NBO basis 3-Acetamidotetrahydro-2-thiophenone.

Electron Localization Function and Localization Orbital (ELF and LOL)

Electron Localization Function and Localization Orbital are modern tools for analyzing electron density distribution in molecular systems [33]. ELF quantifies degree of electron localization, while LOL describes spatial extent of localized electron clouds. Both ELF and

Science Academique
ISSN 2583-6889
Benny D and Prasana JC.
Pages: 47-68

LOL are visualized as color-coded maps in two dimensions.

Figures 6 and 7 depict the ELF and LOL maps of 3-acetamidotetrahydro-2-thiophenone. In ELF map, a deeper blue color indicates a lower electron localization (closer to zero), while red indicates a higher degree of localization (closer to 1.0). In LOL map, blue represents regions of high electron depletion, while red indicates regions of low electron depletion. Analysis of ELF map reveals that hydrogen atoms (H12, H16) in 3-acetamidotetrahydro-2-thiophenone are located in regions of high electron localization (red areas) and Carbon atoms(C6, C7) are in blue region. In LOL map, blue represents regions of high electron depletion, while red indicates regions of low electron depletion. Carbon atoms (C6, C7) are found in blue regions [34].

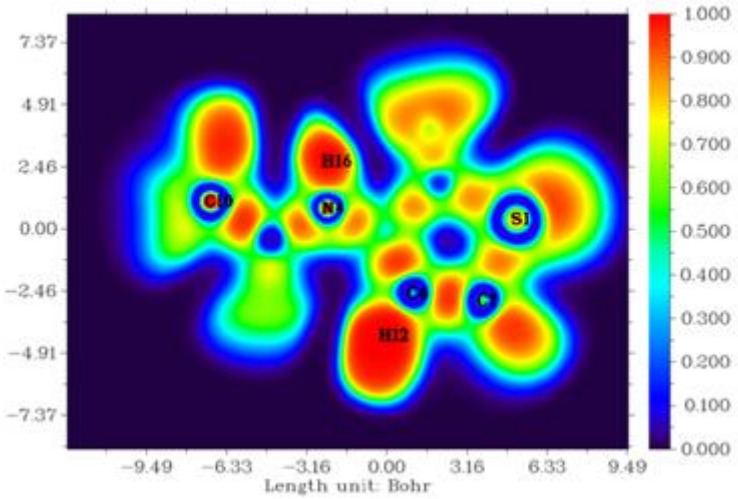

Figure 6: ELF colour-filled map of 3-Acetamidotetrahydro-2-thiophenone.

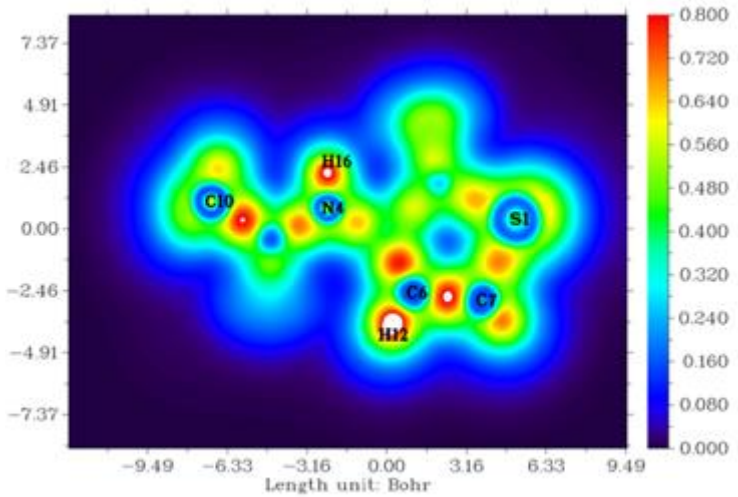

Figure 7: LOL map of 3-Acetamidotetrahydro-2-thiophenone.

Science Academique
ISSN 2583-6889
Benny D and Prasana JC.
Pages: 47-68

Biological Evaluation

Pharmacological studies

Drug-like properties of 3-acetamidotetrahydro-2-thiophenone were evaluated using SwissADME, an online software tool. Adherence to Lipinski's rule is a crucial criterion for selecting potential drug candidates [35]. As shown in Table 6, the compound satisfies all of Lipinski's rules, with an HBD count of 1, an HBA count of 2 (within the preferred range), 3 rotatable bonds (out of a maximum of 10), and a molecular weight of 159.21 g/mol. Calculated drug-likeness parameters fall within the accepted ranges, suggesting that 3-acetamidotetrahydro-2-thiophenone possesses favorable characteristics for drug development [36,37].

Descriptor	value
Hydrogen Bond donors	1
Hydrogen Bond acceptors	2
MlogP	-0.51
GI absorption	high
Lipinski violation	0
skin permeation	-7.52
molar refractivity	39.63
Bioavailability score	0.55
Number of rotatable bonds	3
Molecular weight	159.21 g/mol
BBB permeant	No

Table 6: Drug likeness parameters for 3-acetamido tetrahydro-2-thiophenone compound.

***In vitro* cytotoxicity activity**

3-acetamidotetrahydro-2-thiophenone was tested against the Human Lung Carcinoma (A549) cell line by subjecting the cells to several doses, ranging from 1000µg/mL to 7.8µg/mL. MTT assay was used to measure the metabolic activity using a colorimetric determination to examine the cytotoxic effect of specific doses of the title chemical on the Human Lung Carcinoma (A549) cell line. Since MTT assay is used to identify cells with consistent mitochondrial activity, changes in the number of viable cells are directly correlated with changes in mitochondrial activity. [38]. In the present study, percentage cell viability is given in Table 7 and it was found with 69.62 ± 2.55% cell viability at higher concentration (500µg/mL) on Human Lung Carcinoma (A549) cell line. CTC50 value obtained from MTT assay for the title compound on Human Lung Carcinoma (A549) cells was found to be 855.496 µg/mL. On decreasing concentration, cell viability was found to be increased.

Science Academique
ISSN 2583-6889
Benny D and Prasana JC.
Pages: 47-68

	Concentration (µg/mL)	Percentage of cells viable after treatment
	1000	47.71 ± 4.50
	500	69.62 ± 2.55
3-acetamido tetrahydro-2-thiophenone	250	74.53 ± 3.94
	125	79.11 ± 3.70
	62.5	84.92 ± 2.03
	31.25	90.03 ± 2.13
	15.628	94.64 ± 1.26
	7.8	98.32 ± 0.45

Table 7: Analysis of the in vitro cytotoxicity of 3-acetamido tetrahydro-2-thiophenone against Human Lung Carcinoma (A549) cell line by MTT assay

Ramachandran plot and Molecular docking studies

Ramachandran plots were employed to validate protein structures and assess their binding affinities. Two proteins with anti-emphysema properties, 3NE4 and 3CWL, were selected for docking studies. Ramachandran plots (RC) plots were generated using Discovery Studio software and are depicted in Figures 8 (a) and 8 (b). Only a small number of residues are located in the restricted region. RC plots reveal that majority of amino acid residues in both proteins reside within permitted region of the Ramachandran plot, indicating a stable protein conformation [39,40].

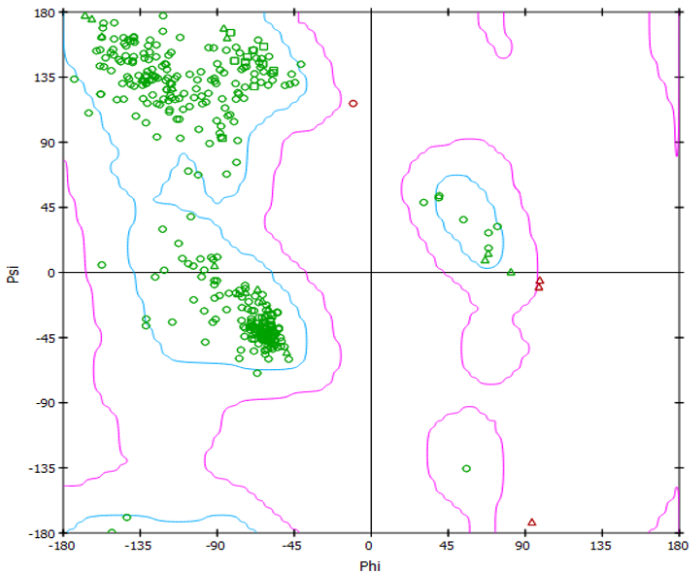

a)3NE4

Science Academique
ISSN 2583-6889
Benny D and Prasana JC.
Pages: 47-68

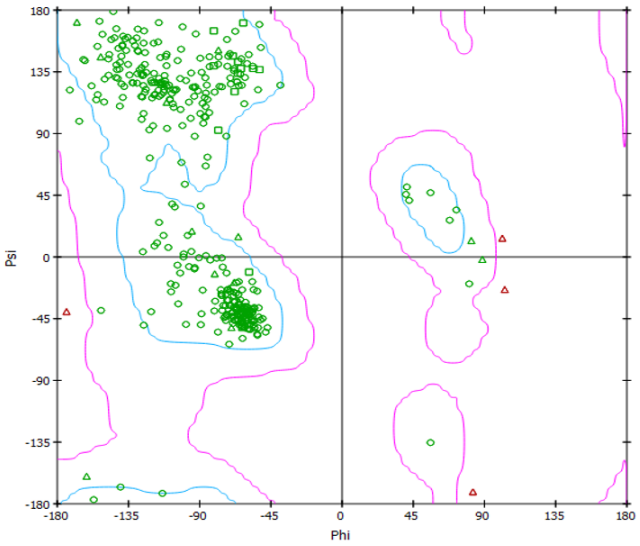

b) 3CWL

Figure 8: Ramachandran plot of proteins.

Molecular docking is a powerful computational technique used to investigate drug-protein interactions [41]. Molecular docking is employed to evaluate the potential therapeutic efficacy of 3-acetamidotetrahydro-2-thiophenone on emphysema. Title compound was docked against the 3NE4 [42] and 3CWL [43] proteins using AutoDock Tools 1.5.6, and resulting ligand-protein interactions were visualized using Discovery Studio. Table 8 summarizes docking results, including binding energies for 3NE4 (-5.14 kcal/mol) and 3CWL (-5.37 kcal/mol). Two-dimensional and three-dimensional representations of ligand-protein interactions are depicted in Figure 9. Glycopyrrolate and Tiotropium bromide are commercially available drugs in treating emphysema and have binding energy -6kcal/mol and -5.7kcal/mol respectively [44]. These findings suggest, 3-acetamidotetrahydro-2-thiophenone exhibits strong anti-emphysema properties [45,46].

Science Academique
ISSN 2583-6889
Benny D and Prasana JC.
Pages: 47-68

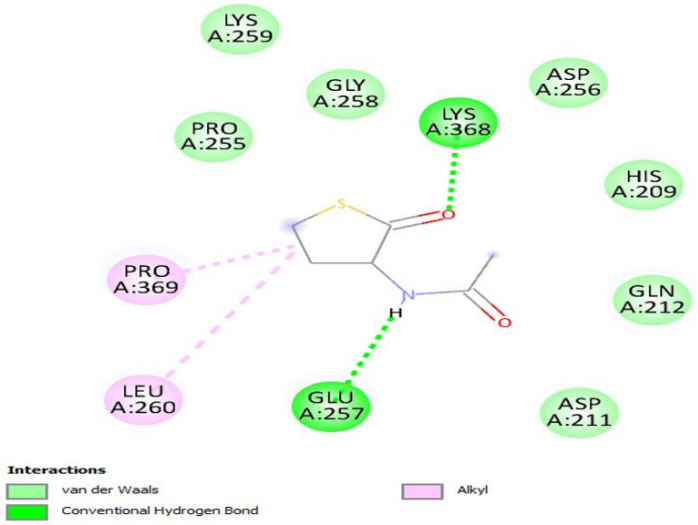

a) 2D docking diagram of 3NE4 and 3-Acetamidotetrahydro-2-thiophenone.

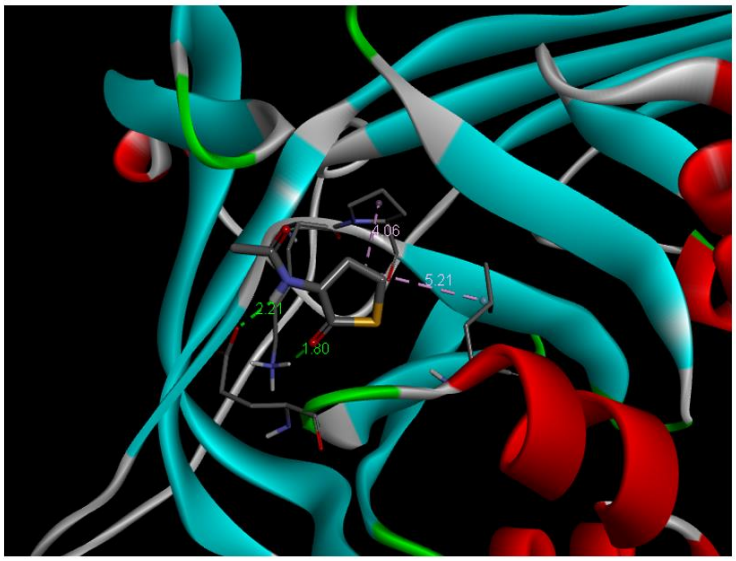

b) 3D molecular docking diagram

Science Academique
ISSN 2583-6889
Benny D and Prasana JC.
Pages: 47-68

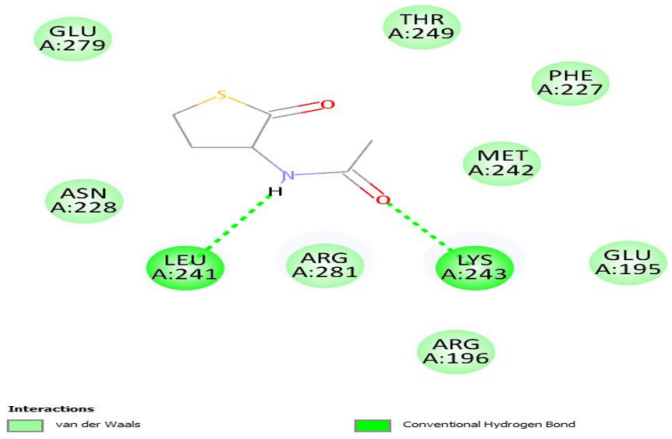

c) 2D docking diagram of 3CWL and 3-Acetamidotetrahydro-2-thiophenone.

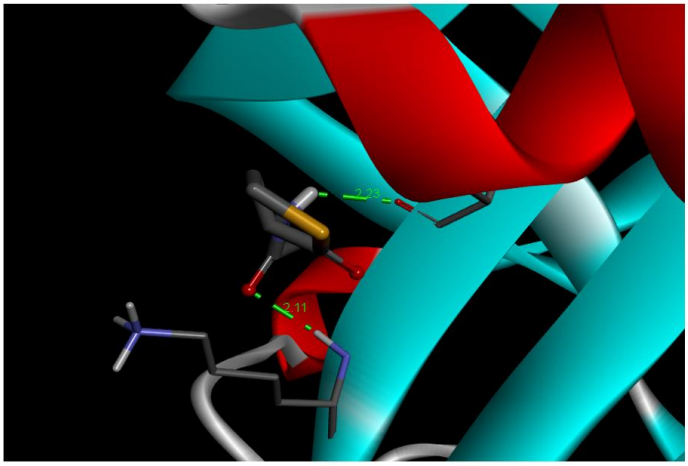

d) 3D molecular docking diagram

Figure 9: 2D and 3D docking diagrams.

Protein (PDB ID)	Bonded residues	Bonded distance(A °)	Type of interaction	Estimated inhibition constant (μM)	Binding energy (kcal/mol)	Reference RMSD(Å)
3NE4	A: LYS368 A: GLU257	1.79 2.20	Conventional Hydrogen Bond Conventional Hydrogen Bond	170.93	-5.14	31.38
	A: LEU260 A:PRO369	5.20 4.06	Alkyl Alkyl			
3CWL	A: LYS243	2.11	Conventional Hydrogen Bond	116.26	-5.37	67.043

Science Academique
ISSN 2583-6889
Benny D and Prasana JC.
Pages: 47-68

	A: LEU241	2.23	Conventional Hydrogen Bond			

Table 8: Molecular docking of 3-acetamidotetrahydro-2-thiophenone.

Conclusion

3-Acetamidotetrahydro-2-thiophenone was subjected to a comprehensive investigation that includes molecular geometry, spectroscopic characterization (FT-IR, FT-Raman), electronic structure analysis (MEP, FMO), Nonlinear Optical Properties (NLO), and biological evaluation. Compound's molecular geometry, vibrational spectra, and electronic transitions were thoroughly explored using both theoretical and experimental approaches. Mapping of molecular electrostatic potential (MEP) provided insights into reactive sites, while frontier molecular orbital (FMO) analysis assessed the compound's stability and reactivity. Additionally, nonlinear optical properties were evaluated, and compound's potential as a drug candidate was assessed using drug likeness criteria. *In vitro* cytotoxicity assays predicted the cell viability of title compound. To explore compound's potential therapeutic applications, molecular docking studies were conducted with proteins associated with emphysema (3NE4 and 3CWL). Binding energies and Ramachandran plots revealed favorable interactions and stability. Binding energy of commercially available drugs (Glycopyrrolate and Tiotropium bromide) was comparable with title compound. Results predict that 3-Acetamidotetrahydro-2-thiophenone could be a promising therapeutic option for the treatment of emphysema.

Disclosure of Interest: The authors report there are no competing interests to declare.

Credit authorship contribution statement

Dona Benny: Validation, Visualization, Writing-original draft, Writing-review and editing.

Johanan Christian Prasana: Validation, Supervision, Resources, Methodology and Software.

References

1. Chaudhary A Jha KK, Kumar S (2012) Biological diversity of thiophene: a review. Journal of Advanced Scientific Research, 3(03), pp.3-10.
2. Shah R, Verma PK (2018) Therapeutic importance of synthetic thiophene. *Chemistry Central Journal,* 12, pp.137.
3. Chen Z, Ku TC, Seley-Radtke KL (2015) Thiophene-expanded guanosine analogues of gemcitabine. *Bioorganic & medicinal chemistry letters*, 25(19), pp.4274-4276.
4. Russell RK, Press JB, Rampulla RA, McNally JJ, Falotico R, Keiser JA, Bright DA, Tobia A (1988) Thiophene systems. 9. Thienopyrimidinedione derivatives as potential antihypertensive agents. *Journal of medicinal chemistry*, 31(9), pp.1786-1793.
5. Pillai AD, Rathod PD, Xavier FP, Padh H, Sudarsanam V, Vasu KK (2005) Tetra substituted thiophenes as anti-inflammatory agents: exploitation of analogue-based drug

Science Academique
ISSN 2583-6889
Benny D and Prasana JC.
Pages: 47-68

design. *Bioorganic & medicinal chemistry*, 13(24), pp.6685-6692.

6. Tehranchian S, Akbarzadeh T, Fazeli MR, Jamalifar H, Shafiee A, (2005) Synthesis and antibacterial activity of 1-[1, 2, 4-triazol-3-yl] and 1-[1, 3, 4-thiadiazol-2-yl]-3-methylthio-6, 7-dihydrobenzo [c] thiophen-4 (5H) ones. *Bioorganic & Medicinal Chemistry Letters*, 15(4), pp.1023-1025.
7. Woodward RB, Eastman RH (1946) Tetrahydrothiophene ("thiophane") derivatives. *Journal of the American Chemical Society*, 68(11), pp.2229-2235.
8. Pathania S, Narang RK, Rawal RK (2019) Role of sulphur-heterocycles in medicinal chemistry: An update. *European journal of medicinal chemistry,* 180, pp.486-508.
9. Frisch MJ, Trucks GW, Schlegel HB, Scuseria GE, Robb MA, et al. (2016) Gaussian16 Revision A. 03 (Wallingford, CT: Gaussian Inc.).
10. Dennington, Roy, Todd Keith, John Millam, Semichem Inc, Shawnee Mission KS, (2009) GaussView, Version 5.
11. Jamróz MH, Vibrational Energy Distribution Analysis; VEDA 4 Program, Warsaw, Poland, 2004–2010.
12. Lu T, Chen F (2012) Multiwfn: A multifunctional wavefunction analyzer. *Journal of computational chemistry*, 33(5), pp.580-592.
13. Filimonov DA, Lagunin AA, Gloriozova TA, Rudik AV, Druzhilovskii DS, et al. (2014) Prediction of the biological activity spectra of organic compounds using the PASS online web resource. *Chemistry of Heterocyclic Compounds*, 50, pp.444-457.
14. The PyMOL Molecular Graphics Development Component, Version 1.8, PYMOL Mol. Graph. Dev. Component,Version 1.8, Schrodinger LLC.
15. Dassault Systemes BIOVIA: Discovery Studio Visualizer 21.1.0.20298, 2020.
16. Priscilla J, Dhas DA, Joe IH, Balachandran S, (2020) Experimental and theoretical spectroscopic analysis, hydrogen bonding, reduced density gradient and antibacterial activity study on 2-Phenyl quinoline alkaloid. *Chemical Physics*, 536, p.110827.
17. Benny D, Prasana JC, Thirunavukkarasu M, Khaled JM, Muthu S, (2024) In vitro cytotoxicity activity (MTT assay), Experimental spectral investigations, Quantum Computational, Solvents performance, and biological evaluation on N-tert-Butoxycarbonylimidazole. *Journal of the Indian Chemical Society*, p.101366.
18. Anju LS, Aruldhas D, Joe IH, John NL (2020) Spectroscopic, quantum mechanical and docking studies on organochlorine insecticides by density functional theory. *Journal of Molecular Structure*, 1208, p.127904.
19. Colthup NB, Daly LH, Wiberley SE (1990) AMINES, C= N, AND N= O COMPOUNDS. Introduction to infrared and Raman spectroscopy, pp.339-354.
20. Tanak H, Marchewka MK (2013) FT-IR, FT-Raman, and DFT computational studies of melaminium nitrate molecular–ionic crystal. *Journal of Molecular Structure*, 1034, pp.363-373.
21. Edwin B, Joe IH (2013) Vibrational spectral analysis of anti-neurodegenerative drug Levodopa: A DFT study. *Journal of Molecular Structure*, 1034, pp.119-127.
22. Udhayakala P, Rajendiran TV, Seshadri S, Gunasekaran S (2011) Quantum chemical vibrational study, molecular property and HOMO-LUMO energies of 3-bromoacetophenone for Pharmaceutical application. *J. Chem. Pharm. Res*, 3(3), pp.610-625.
23. Amalanathan M, Suresh DM, Joe IH, Jothy VB, Sebastian S, Ayyapan S (2016) FT-IR and

Science Academique
ISSN 2583-6889
Benny D and Prasana JC.
Pages: 47-68

FT-Raman spectral investigation and DFT computations of pharmaceutical important molecule: ethyl 2-(4-Benzoyl-2, 5-dimethylphenoxy) acetate. *Pharm Anal Acta*, 7(457), pp.26-28.

24. Satheeshkumar K, Kumar PS, Shanmugapriya R, Nandhini C, Vennila KN, Elango KP (2023) Ratiometric fluorescence sensing of hypochlorite ion by dansyl hydrazine-Spectroscopic and TD-DFT studies. *Journal of Molecular Structure*, 1275, p.134719.

25. Kumer A, Sarker MN, Paul S (2019) The simulating study of HOMO, LUMO, thermo physical and quantitative structure of activity relationship (QSAR) of some anticancer active ionic liquids. *Eurasian Journal of Environmental Research*, 3(1), pp.1-10.

26. Çalışkan ŞG, Genç O, Erol F, Sarıkavaklı N (2022) Molecular Docking, HOMO-LUMO, Quantum Chemical Computation and Bioactivity Analysis of vic-Dioxim Derivatives Bearing Hydrazone Group Ligand and Their NiII and CuII Complexes. Gazi University *Journal of Science Part A: Engineering and Innovation*, 9(3), pp.299-313.

27. Gadre SR, Kulkarni SA, Shrivastava IH (1992) Molecular electrostatic potentials: A topographical study. *The Journal of chemical physics*, 96(7), pp.5253-5260.

28. Murray JS, Sen K, eds., (1996) Molecular electrostatic potentials: concepts and applications.

29. Pallen S, Shetty Y, Das S, et al. (2021) Advances in nonlinear optical microscopy techniques for in vivo and in vitro neuroimaging, *Biophys. Rev.* 13: 1199–1217.

30. Zhang S, Liu L, Ren S, Li Z, Zhao Y, et al. (2020) Recent advances in nonlinear optics for bio-imaging applications, *Opto-Electron. Adv*. 3: 200003.

31. Gangadharan R, Sampath Krishnan S (2014) Natural Bond Orbital (NBO) population analysis of 1-azanapthalene-8-ol. *Acta Physica Polonica* A, 125(1), pp.18-22.

32. Snehalatha M, Ravikumar C, Joe IH, Sekar N, Jayakumar VS (2009) Spectroscopic analysis and DFT calculations of a food additive Carmoisine. *Spectrochimica Acta Part A: Molecular and Biomolecular Spectroscopy*, 72(3), pp.654-662.

33. Arulaabaranam K, Muthu S, Mani G, Geoffrey AB. Speculative assessment, molecular composition. PDOS, topology exploration (ELF, LOL, RDG), ligand-protein interactions, on.

34. Tarika JD, Dexlin XD, Madhankumar S, Jayanthi DD, Beaula TJ (2021) Tuning the computational evaluation of spectroscopic, ELF, LOL, NCI analysis and molecular docking of novel antiCOVID-19 molecule 4-dimethylamino pyridinium 3, 5-dichlorosalicylate. Spectrochimica Acta Part A: Molecular and Biomolecular Spectroscopy, 259, p.119907.

35. Mumit MA, Pal TK, Alam MA, Islam MAAAA, Paul S, Sheikh MC (2020) DFT studies on vibrational and electronic spectra, HOMO–LUMO, MEP, HOMA, NBO and molecular docking analysis of benzyl-3-N-(2, 4, 5-trimethoxyphenylmethylene) hydrazinecarbodithioate. Journal of molecular structure, 1220, p.128715.

36. Tian S, Wang J, Li Y, Li D, Xu L, Hou T (2015) The application of in silico drug-likeness predictions in pharmaceutical research. *Advanced drug delivery reviews*, 86, pp.2-10.

37. Lipinski CA, (2004) Lead-and drug-like compounds: the rule-of-five revolution. *Drug discovery today: Technologies*, 1(4), pp.337-341.

38. Denizot F, Lang R (1986) Rapid colorimetric assay for cell growth and survival: modifications to the tetrazolium dye procedure giving improved sensitivity and

Science Academique
ISSN 2583-6889
Benny D and Prasana JC.
Pages: 47-68

reliability. *Journal of immunological methods*, 89(2), pp.271-277.

39. Benny D, Prasana JC, Khaled JM, Abbas G, Muthu S (2023) Experimental, computational investigations and biological evaluation on 1-(3-acetamidophenyl)-5-mercaptotetrazole-cytotoxicity MTT assay. *Journal of Molecular Liquids*, 389, p.122903.

40. Bathula R, Muddagoni N, Lanka G, Dasari M, Potlapally S (2021) Glide docking, autodock, binding free energy and drug-likeness studies for prediction of potential inhibitors of cyclin-dependent kinase 14 protein in wnt signaling pathway. *Biointerface Res Appl Chem*, 12(2), pp.2473-2488.

41. Kumar M, Ahmad S, Garima K, Ali A, Arora H, Muthu S, Saral A, Kumar A, Afzal M, Javed S (2023) Molecular docking and dynamic simulations of 2-phenoxyaniline and quantum computational, spectroscopic, DFT/TDDFT investigation of electronic states in various solvents. *Chemical Physics Impact*, 7, p.100307.

42. Angstrom structure of intact native wild-type alpha-1-antitrypsin.

43. Crystal structure of alpha-1-antitrypsin, crystal form B.

44. Wong B, Datla SSP, Li C, Joyce C, Alzagatiti J, Developing anticholinergic drugs for the treatment of asthma with improved efficacy.

45. Gopi B, Vijayakumar V (2024) Synthesis and molecular docking of novel indazole derivatives with DFT studies.

46. Hamzah HA, Afladhanti PM, Romadhan MD, Agustini D, Deanasa RS (2022) Molecular Docking of Mangrove Plant as Therapeutic Agent to Treat Non-Small Cell Lung Carcinoma. *Journal of Pharmaceutical Research International*, 34(46A), pp.30-39.